

# Polynomial Approximants for the Calculation of Polarization Profiles in the He I 10830 Å Multiplet

H. Socas-Navarro

*High Altitude Observatory, NCAR<sup>1</sup>, 3450 Mitchell Lane, Boulder, CO 80307-3000, USA*  
 navarro@ucar.edu

J. Trujillo Bueno <sup>2</sup>

*Instituto de Astrofísica de Canarias, Avda Vía Láctea S/N, La Laguna 38205, Tenerife, Spain*  
 jtb@iac.es

E. Landi Degl’Innocenti

*Dipartimento di Astronomia e Scienza dello Spazio, Largo E. Fermi 2, 50125 Firenze, Italy*  
 landie@arcetri.astro.it

## ABSTRACT

The He I multiplet at 10830 Å is formed in the incomplete Paschen-Back regime for typical conditions found in solar and stellar atmospheres. The positions and strengths of the various components that form the Zeeman structure of this multiplet in the Paschen-Back regime are approximated here by polynomials. The fitting errors are smaller than  $\sim 10^{-2}$  mÅ in the component positions and  $\sim 10^{-3}$  in the relative strengths. The approximant polynomials allow for a very fast implementation of the incomplete Paschen-Back regime in numerical codes for the synthesis and inversion of polarization profiles in this important multiplet.

*Subject headings:* line: profiles – Sun: atmosphere – Sun: magnetic fields – Sun: chromosphere

## 1. Introduction

One of the most useful near-infrared spectral regions for spectropolarimetric investigations of solar and stellar magnetic fields is that located around 10830 Å, which contains both the photospheric line of Si I at 10827 Å and the chromospheric lines that result from the He I 10830 Å multiplet (Harvey & Hall 1971; Rüedi et al. 1995; Trujillo Bueno et al. 2002). Of particular interest is the fact that the ‘blue’ and ‘red’ components of this multiplet are sensitive to both the Hanle and Zeeman effects, which offers a suitable diagnostic window for investigating magnetic fields in

a variety of solar plasma structures, such as prominences (Trujillo Bueno et al. 2002), emerging flux regions (Solanki et al. 2003) and solar chromospheric spicules (Trujillo Bueno et al. 2005; Socas-Navarro & Elmore 2005). The He I 10830 Å multiplet originates between a lower term ( $2^3S_1$ ) and an upper term ( $2^3P_{2,1,0}$ ). Therefore, it comprises three spectral lines (see, e.g., Radzig & Smirnov 1985): a ‘blue’ component at 10829.09 Å with  $J_l = 1$  and  $J_u = 0$  (hereafter Transition 1, or Tr1 for abbreviation), and two ‘red’ components at 10830.25 Å with  $J_u = 1$  (hereafter, Tr2) and at 10830.34 Å with  $J_u = 2$  (hereafter, Tr3) which appear blended at solar atmospheric temperatures.

In a previous paper (Socas-Navarro et al. 2004, hereafter paper-I), we demonstrated that the determination of the magnetic field vector via the

<sup>1</sup>The National Center for Atmospheric Research (NCAR) is sponsored by the National Science Foundation.

<sup>2</sup>Consejo Superior de Investigaciones Científicas, Spain

analysis of the observed polarization in the He I 10830 Å multiplet must be carried out considering the wavelength positions and the strengths of the Zeeman components in the incomplete Paschen-Back effect regime. The theory of the Paschen-Back effect in this regime is detailed in Section 3.4 of the book by Landi Degl’Innocenti & Landolfi (2004). The problem of finding the strengths and the splittings of the various magnetic components, arising in the transition from a lower and an upper term, both described in the L-S coupling scheme ( $^3S$  and  $^3P$ , respectively, in the case of the  $\lambda 10830$  line), is reduced to the numerical diagonalization of a number of matrices. The expressions of the matrix elements are given, in terms of Wigner-symbols, in Eq. (3.57) of that book, or, in analytical form, in Eqs. (3.61a,b). As pointed out in paper-I, our results have been obtained through the adaptation to the fine-structure case of a computer program previously developed to handle the similar problem for hyperfine-structured multiplets (Landi Degl’Innocenti 1978).

Fig 1 shows the transition components with the linear Zeeman splitting (LZS) approximation and the rigorous calculation considering the incomplete Paschen-Back splitting effects (IPBS). The figure has been reproduced from paper-I, but corrects a plotting error in one of the Tr3  $\pi$ -components.

Significant differences between LZS and IPBS are to be expected for typical magnetic strengths in sunspots, simply because for fields stronger than about 400 gauss the Zeeman splittings of the  $J = 2$  and  $J = 1$  levels of the upper term become comparable to their energy separation and the perturbation theory of the familiar Zeeman effect is no longer valid. However, the discrepancies between the emergent Stokes profiles calculated assuming LZS or IPBS turn out to be significant even for field strengths substantially weaker than the level-crossing field of  $\sim 400$  G (see paper-I).

In this paper we provide polynomial approximants that allow researchers to calculate Zeeman components and strengths of this interesting multiplet in the IPBS regime. This will facilitate the generalization of numerical codes developed with the LZS approximation, such as the Milne-Eddington code of Lagg et al. 2004, and to improve the efficiency of the IPBS code of Socas-Navarro et al (2004). Moreover, it may also be

useful for solving the full non-LTE polarization transfer problem in the He I 10830 Å multiplet within the framework of the incomplete Paschen-Back effect theory.

Figure 2 demonstrates that our polynomial approach to the IPBS regime in the He I 10830 Å multiplet is sufficiently accurate for the calculation of the emergent Stokes profiles from a magnetized stellar atmosphere.

## 2. Polynomial fits

Let us characterize the deviation of the Zeeman pattern from the LZS as polynomials. For each Zeeman component, we have:

$$\begin{aligned}\Delta\lambda_{IPB} &= \Delta\lambda_{LZS} + y_p(x) \\ f_{IPB} &= f_{LZS} + y_f(x),\end{aligned}\quad (1)$$

where  $\Delta\lambda$  denotes the relative position of a given component (in mÅ),  $f$  represents the relative strengths which are dimensionless quantities (see, e.g., Eq [3.64] in Landi Degl’Innocenti & Landolfi 2004),  $x$  is the magnetic field intensity expressed in kG, and  $y(x)$  are the approximant polynomials. Since the expressions for the splittings and the strengths in the IPBS regime have to converge to those of the LZS effect under the limit of weak fields, and since, under the same limit, the splittings are linear in the magnetic field and the strengths tend to a constant, it has to be expected that the differences  $y_p$  and  $y_f$  are of the form:

$$\begin{aligned}y_p &= c_2x^2 + c_3x^3 + c_4x^4 + c_5x^5 \\ y_f &= d_1x + d_2x^2 + d_3x^3 + d_4x^4,\end{aligned}\quad (2)$$

with  $0 < x < 3$ .

The following tables list the coefficients for the corrections  $y_p(x)$  and  $y_f(x)$  that need to be applied to the LZS approximation to account for IPB effects. The last column of each table lists the maximum fitting error in the range considered ( $0 < x < 3$ ). The components are sorted in the order of increasing wavelengths in the LZS regime.

## 3. Conclusions

The polynomial coefficients provided in this work can be used to generalize existing Zeeman transfer codes to treat the He I 10830 Å multiplet in the IPBS regime. As we pointed out in a

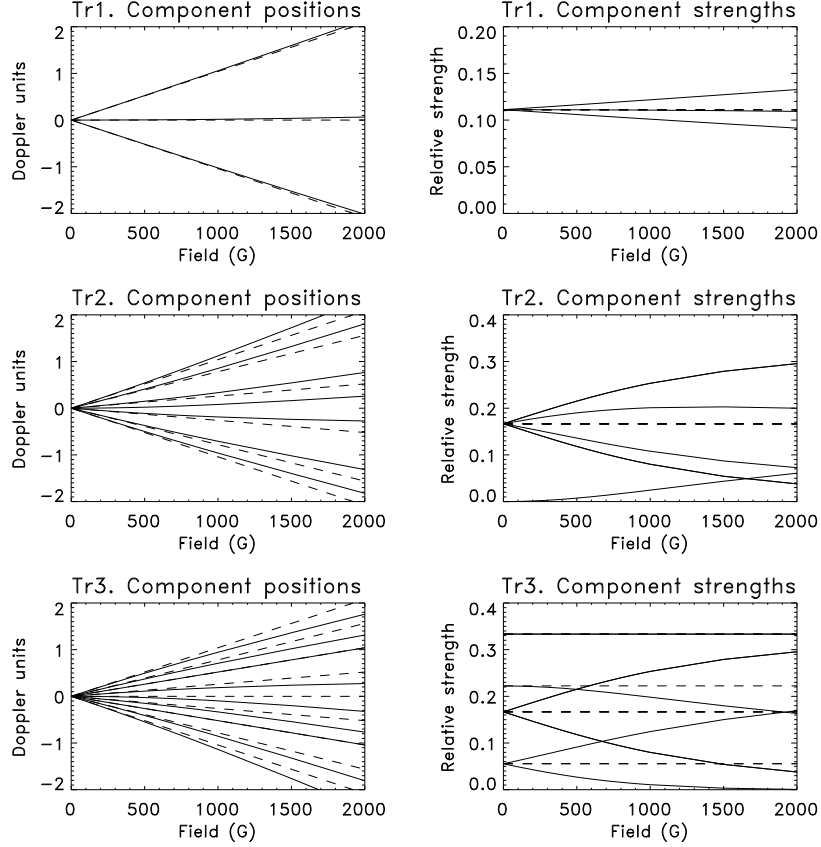


Fig. 1.— Positions and strengths of the Zeeman components as a function of the magnetic field. In all panels the solid lines represent calculations considering IPBS while the dashed lines represent those using the LZS approximation. Note that, in the general IPBS case, the Zeeman components exhibit asymmetric displacements and strengths. Also notice that the Zeeman IPBS components have strengths that depend on the magnetic field. The central  $\pi$ -component of Tr2 has zero strength in LZS and is not plotted in the figure. The ordinate axes are given in Doppler units (corresponding to 105 mÅ) to make the figure directly comparable with that in paper-I.

TABLE 1  
COMPONENT POSITIONS. TR1

Transition	$c_2$	$c_3$	$c_4$	$c_5$	Max error
$\sigma^+$	1.685	$3.072 \times 10^{-2}$	$-1.366 \times 10^{-2}$	$1.568 \times 10^{-3}$	$4.508 \times 10^{-3}$
$\pi$	1.685	$3.073 \times 10^{-2}$	$-1.366 \times 10^{-2}$	$1.567 \times 10^{-3}$	$4.505 \times 10^{-3}$
$\sigma^-$	1.685	$3.073 \times 10^{-2}$	$-1.366 \times 10^{-2}$	$1.567 \times 10^{-3}$	$4.505 \times 10^{-3}$

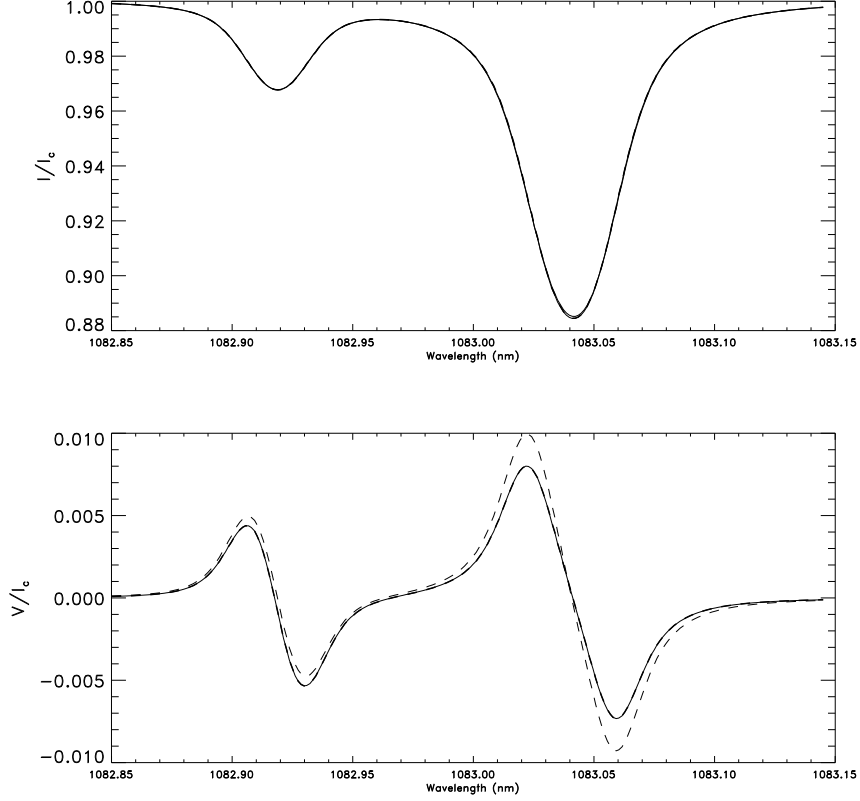


Fig. 2.— Stokes I and V profiles calculated according to a Milne-Eddington atmosphere for a 500 G field. Solid line: Strict IPBS calculation. Thin dashed line: LZS approximation. Thick dashed line: LZS corrected with the coefficients provided in this paper. The error induced by this approximation on the synthetic profiles is smaller than  $\sim 10^{-4}$  and is hardly noticeable in the figure.

TABLE 2  
COMPONENT STRENGTHS. TR1

Transition	$d_1$	$d_2$	$d_3$	$d_4$	Max error
$\sigma^+$	$-1.040 \times 10^{-2}$	$2.326 \times 10^{-4}$	$1.577 \times 10^{-5}$	$-8.117 \times 10^{-7}$	$6.836 \times 10^{-7}$
$\pi$	$-1.280 \times 10^{-7}$	$-4.635 \times 10^{-4}$	$2.127 \times 10^{-8}$	$1.606 \times 10^{-6}$	$1.034 \times 10^{-7}$
$\sigma^-$	$1.040 \times 10^{-2}$	$2.331 \times 10^{-4}$	$-1.740 \times 10^{-5}$	$-4.781 \times 10^{-7}$	$8.643 \times 10^{-7}$

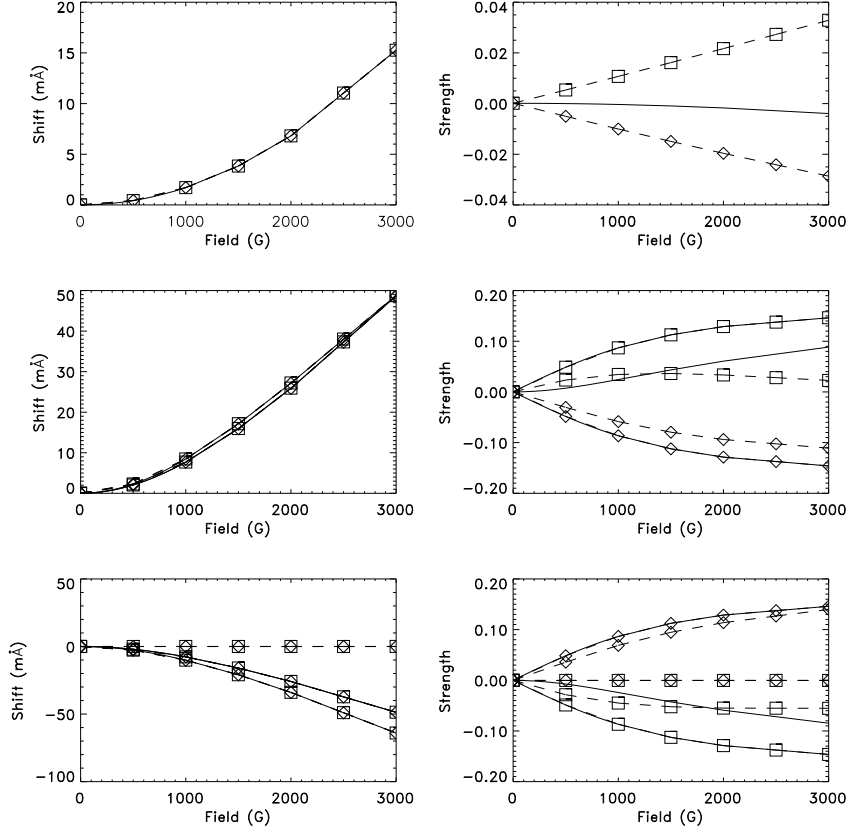


Fig. 3.— Difference between IPBS and LZS component. Left panels: Position shifts ( $\Delta\lambda_{IPB} - \Delta\lambda_{LZS}$ ). Right panels: Relative strengths ( $f_{IPB} - f_{LZS}$ ). Top to bottom: Tr1, Tr2 and Tr3. In all panels, the solid lines represent  $\pi$ -components and the dashed lines represent  $\sigma$ -components (diamonds:  $\sigma^+$ , squares:  $\sigma^-$ ).

TABLE 3  
COMPONENT POSITIONS. TR2

Transition	$c_2$	$c_3$	$c_4$	$c_5$	Max error
$\sigma^+$	8.477	$-4.631 \times 10^{-1}$	$-4.402 \times 10^{-1}$	$8.436 \times 10^{-2}$	$9.841 \times 10^{-3}$
$\sigma^+$	9.678	$-8.777 \times 10^{-1}$	$-4.968 \times 10^{-1}$	$1.052 \times 10^{-1}$	$1.569 \times 10^{-2}$
$\pi$	8.556	$-5.492 \times 10^{-1}$	$-4.028 \times 10^{-1}$	$7.882 \times 10^{-2}$	$8.270 \times 10^{-3}$
$\pi$	9.757	$-9.627 \times 10^{-1}$	$-4.601 \times 10^{-1}$	$9.984 \times 10^{-2}$	$1.419 \times 10^{-2}$
$\pi$	8.517	$-5.067 \times 10^{-1}$	$-4.212 \times 10^{-1}$	$8.153 \times 10^{-2}$	$9.087 \times 10^{-3}$
$\sigma^-$	9.835	-1.049	$-4.226 \times 10^{-1}$	$9.430 \times 10^{-2}$	$1.264 \times 10^{-2}$
$\sigma^-$	8.596	$-5.927 \times 10^{-1}$	$-3.839 \times 10^{-1}$	$7.602 \times 10^{-2}$	$7.527 \times 10^{-3}$

TABLE 4  
COMPONENT STRENGTHS. TR2

Transition	$d_1$	$d_2$	$d_3$	$d_4$	Max error
$\sigma^+$	$-1.019 \times 10^{-1}$	$4.219 \times 10^{-3}$	$1.334 \times 10^{-2}$	$-2.952 \times 10^{-3}$	$1.464 \times 10^{-3}$
$\sigma^+$	$-5.746 \times 10^{-2}$	$-1.458 \times 10^{-2}$	$1.583 \times 10^{-2}$	$-2.904 \times 10^{-3}$	$1.014 \times 10^{-3}$
$\pi$	$1.019 \times 10^{-1}$	$-4.220 \times 10^{-3}$	$-1.334 \times 10^{-2}$	$2.952 \times 10^{-3}$	$1.464 \times 10^{-3}$
$\pi$	$-2.566 \times 10^{-4}$	$3.714 \times 10^{-2}$	$-1.443 \times 10^{-2}$	$1.785 \times 10^{-3}$	$4.085 \times 10^{-4}$
$\pi$	$-1.019 \times 10^{-1}$	$4.219 \times 10^{-3}$	$1.334 \times 10^{-2}$	$-2.952 \times 10^{-3}$	$1.464 \times 10^{-3}$
$\sigma^-$	$5.772 \times 10^{-2}$	$-2.256 \times 10^{-2}$	$-1.398 \times 10^{-3}$	$1.118 \times 10^{-3}$	$1.422 \times 10^{-3}$
$\sigma^-$	$1.019 \times 10^{-1}$	$-4.220 \times 10^{-3}$	$-1.334 \times 10^{-2}$	$2.952 \times 10^{-3}$	$1.464 \times 10^{-3}$

TABLE 5  
COMPONENT POSITIONS. TR3

Transition	$c_2$	$c_3$	$c_4$	$c_5$	Max error
$\sigma^+$	$-1.603 \times 10^{-2}$	$4.348 \times 10^{-3}$	$6.113 \times 10^{-4}$	$-2.495 \times 10^{-4}$	$3.138 \times 10^{-3}$
$\sigma^+$	-8.602	$5.997 \times 10^{-1}$	$3.807 \times 10^{-1}$	$-7.555 \times 10^{-2}$	$7.403 \times 10^{-3}$
$\sigma^+$	-11.550	1.059	$4.188 \times 10^{-1}$	$-9.351 \times 10^{-2}$	$1.242 \times 10^{-2}$
$\pi$	-8.516	$5.064 \times 10^{-1}$	$4.214 \times 10^{-1}$	$-8.157 \times 10^{-2}$	$9.046 \times 10^{-3}$
$\pi$	-11.470	$9.645 \times 10^{-1}$	$4.605 \times 10^{-1}$	$-9.970 \times 10^{-2}$	$1.410 \times 10^{-2}$
$\pi$	-8.558	$5.517 \times 10^{-1}$	$4.017 \times 10^{-1}$	$-7.866 \times 10^{-2}$	$8.149 \times 10^{-3}$
$\sigma^-$	-11.380	$8.720 \times 10^{-1}$	$5.007 \times 10^{-1}$	$-1.056 \times 10^{-1}$	$1.577 \times 10^{-2}$
$\sigma^-$	-8.474	$4.600 \times 10^{-1}$	$4.415 \times 10^{-1}$	$-8.453 \times 10^{-2}$	$9.867 \times 10^{-3}$
$\sigma^-$	$1.566 \times 10^{-2}$	$-4.191 \times 10^{-3}$	$-5.948 \times 10^{-4}$	$2.399 \times 10^{-4}$	$2.909 \times 10^{-3}$

TABLE 6  
COMPONENT STRENGTHS. TR3

Transition	$d_1$	$d_2$	$d_3$	$d_4$	Max error
$\sigma^+$	0.000	0.000	0.000	0.000	0.000
$\sigma^+$	$1.019 \times 10^{-1}$	$-4.220 \times 10^{-3}$	$-1.334 \times 10^{-2}$	$2.952 \times 10^{-3}$	$1.463 \times 10^{-3}$
$\sigma^+$	$6.786 \times 10^{-2}$	$1.435 \times 10^{-2}$	$-1.584 \times 10^{-2}$	$2.904 \times 10^{-3}$	$1.012 \times 10^{-3}$
$\pi$	$-1.019 \times 10^{-1}$	$4.220 \times 10^{-3}$	$1.334 \times 10^{-2}$	$-2.952 \times 10^{-3}$	$1.464 \times 10^{-3}$
$\pi$	$2.606 \times 10^{-4}$	$-3.669 \times 10^{-2}$	$1.444 \times 10^{-2}$	$-1.789 \times 10^{-3}$	$4.060 \times 10^{-4}$
$\pi$	$1.019 \times 10^{-1}$	$-4.220 \times 10^{-3}$	$-1.334 \times 10^{-2}$	$2.952 \times 10^{-3}$	$1.463 \times 10^{-3}$
$\sigma^-$	$-6.812 \times 10^{-2}$	$2.232 \times 10^{-2}$	$1.415 \times 10^{-3}$	$-1.117 \times 10^{-3}$	$1.422 \times 10^{-3}$
$\sigma^-$	$-1.019 \times 10^{-1}$	$4.220 \times 10^{-3}$	$1.334 \times 10^{-2}$	$-2.952 \times 10^{-3}$	$1.464 \times 10^{-3}$
$\sigma^-$	0.000	0.000	0.000	0.000	0.000

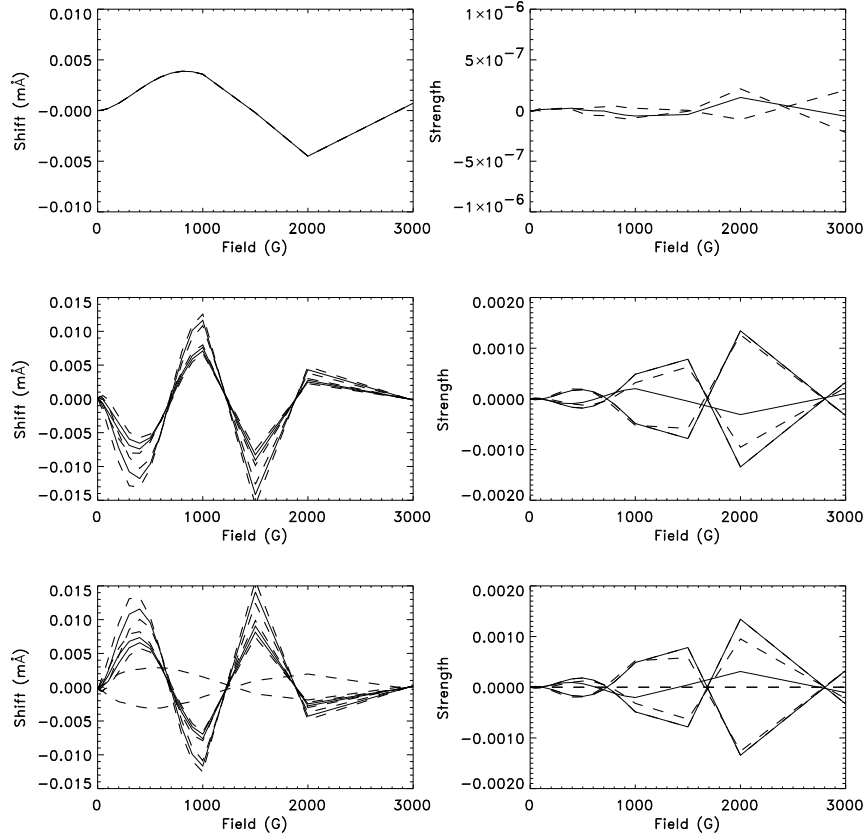


Fig. 4.— Approximation errors. Left panels: Position shifts  $[(\Delta\lambda_{IPB} - \Delta\lambda_{LZS}) - y_p]$ . Right panels: Relative strengths  $[(f_{IPB} - f_{LZS}) - y_f]$ . Top to bottom: Tr1, Tr2 and Tr3. In all panels, the solid lines represent  $\pi$ -components and the dashed lines represent  $\sigma$ -components.

previous work (Socas-Navarro et al 2004), neglecting IPBS results in significant errors in the calculation of its polarization profiles, even for field strengths much lower than the level-crossing field. Computer codes developed using these polynomials will be virtually as fast as those using the LZS approximation but the polarization profiles will be much more accurate. The actual improvement in CPU time obviously depends on the particular details of the calculation. In our codes, the use of the polynomials is approximately a factor 20 faster than the full IPBS implementation.

This research has been partly funded by the Ministerio de Educación y Ciencia through project AYA2004-05792 and by the European Solar Magnetism Network (contract HPRN-CT-2002-00313).

## REFERENCES

- Harvey, J., & Hall, D. 1971, in IAU Symp. 43: Solar Magnetic Fields, 279–+
- Lagg, A., Woch, J., Krupp, N., & Solanki, S. K. 2004, A&A, 414, 1109
- Landi Degl’Innocenti, E. 1978, A&AS, 33, 157
- Landi Degl’Innocenti, E., & Landolfi, M. 2004, Polarization in Spectral Lines (Kluwer Academic Publishers)
- Rüedi, I., Solanki, S. K., & Livingston, W. C. 1995, A&A, 293, 252
- Radzig, A. A., & Smirnov, B. M. 1985, Reference data on Atoms, Molecules and Ions (Springer, Berlin)
- Socas-Navarro, H., & Elmore, D. 2005, ApJ, 619, L195
- Socas-Navarro, H., Trujillo Bueno, J., & Landi Degl’Innocenti, E. 2004, ApJ, 612, 1175
- Solanki, S. K., Lagg, A., Woch, J., Krupp, N., & Collados, M. 2003, Nature, 425, 692
- Trujillo Bueno, J., Landi Degl’Innocenti, E., Collados, M., Merenda, L., & Manso Sainz, R. 2002, Nature, 415, 403
- Trujillo Bueno, J., Merenda, L., Centeno, R., Collados, M., & Landi Degl’Innocenti, E. 2005, ApJ, 619, L191